VIP Supramolecular Chemistry Very Important Paper

International Edition: DOI: 10.1002/anie.201501321
German Edition: DOI: 10.1002/ange.201501321

High-Fidelity Noncovalent Synthesis of Hydrogen-Bonded Macrocyclic Assemblies**

*Carlos Montoro-García, Jorge Camacho-García, Ana M. López-Pérez, Nerea Bilbao, Sonia Romero-Pérez, María J. Mayoral, and David González-Rodríguez**

Abstract: *A hydrogen-bonded cyclic tetramer is assembled with remarkably high effective molarities from a properly designed dinucleoside monomer. This self-assembled species exhibits an impressive thermodynamic and kinetic stability and is formed with high fidelities within a broad concentration range.*

Noncovalent synthesis comprises the spontaneous generation of a well-defined structure from a set of molecular components bound by supramolecular interactions.[1] The understanding and application of this concept to discrete macrocyclic architectures is very appealing, not only because of their stimulating structure, but also because of their manifold possibilities.[2] Self-assembled macrocycles[3] offer low synthetic efforts and high versatilities, but[2a,4] as they are built from the interplay of multiple weak interactions operating under thermodynamic equilibrium, they do not enjoy the persistency and robustness of their covalent analogues. Additionally, achieving complete selectivity (i.e., high fidelity) towards the target cyclic structure is a challenging task which demands careful molecular design.

Key in this design is the optimization of chelate cooperativity,[5] which is also responsible for many of the "all-or-nothing" molecular assembly processes in biological systems.[6] It originates from the fact that an intramolecular association event (i.e., ring closure) is favored over an intermolecular one because it does not involve a high translational and rotational entropy loss. The equilibrium constant ratio K_{intra}/K_{inter} is defined as the effective molarity (EM) of the system,[7] and is used to quantify the chelate effect.[8] The maximization of EM for a given macrocycle is therefore essential to reach high yields over "open" oligomers, on one hand, and over other undesired cyclic structures, on the other (Figure 1 a).[9] The enthalpic term of EM is mainly correlated with the strain generated upon cyclization and can be thus optimized by preorganization of the monomer structure so that the binding interaction produces the target cyclic assembly devoid of strain. The entropic term encompasses the loss of conformational degrees of freedom upon cyclization and is often related to the number and nature of rotatable bonds present in the monomer. Hence, rigid monomers with low conformational freedom are preferable. Entropy is also responsible for the notable decay in EM values as the cyclic assembly is built from more molecules.

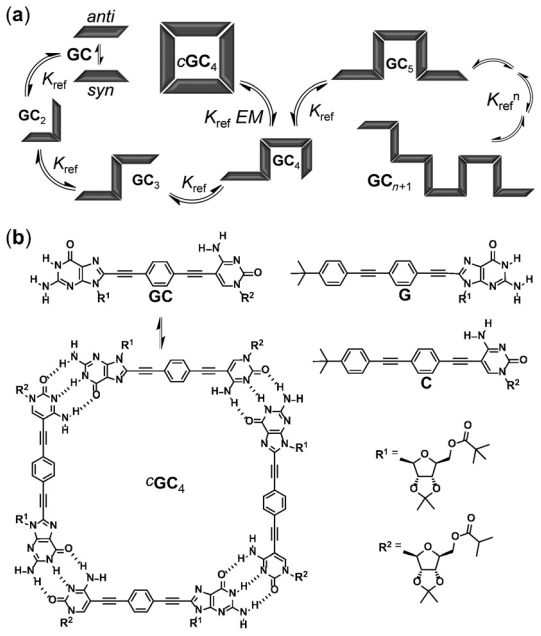

Figure 1. a) Self-assembly of a ditopic monomer (**GC**) to yield cyclic (c**GC**$_4$) or linear oligomeric (**GC**$_{n+1}$) species. b) Chemical structures of **GC**, **G**, and **C**, which are studied herein,[14] as well as the cyclic tetramer c**GC**$_4$.

Here, we focus on the study of a ditopic monomer (**GC**; Figure 1 b) which has been designed to yield cyclic tetramer[10] hydrogen-bonded assemblies[11] with high EM values. **GC** comprises complementary guanosine (G) and cytidine (C) nucleosides[12] at both edges, and have bulky lipophilic groups at the ribose to afford solubility and prevent stacking[13] so that we can only focus on the study of the hydrogen-bonding process in solution. It is essential to note that, upon Watson–Crick pairing, the 5C position and the 8G position form an angle of 90°. We have linked those positions in **GC** through a rigid, linear, and π-conjugated *p*-diethynylbenzene block so that three hydrogen-bonding interactions between complementary bases afford an unstrained square-shaped assembly (c**GC**$_4$) with minimal entropic cost. In this work, we have devised several experiments that demonstrate the consequen-

[*] C. Montoro-García, J. Camacho-García, Dr. A. M. López-Pérez, N. Bilbao, S. Romero-Pérez, Dr. M. J. Mayoral, Dr. D. González-Rodríguez
Nanostructured Molecular Systems and Materials group
Departamento de Química Orgánica, Facultad de Ciencias
Universidad Autónoma de Madrid, 28049 Madrid (Spain)
E-mail: david.gonzalez.rodriguez@uam.es

[**] Funding from MINECO (CTQ2011-23659) and the E.U. (ERC-Starting Grant 279548) is gratefully acknowledged.

Supporting information for this article is available on the WWW under http://dx.doi.org/10.1002/anie.201501321.

ces of a suitable monomer design in the fidelity of the self-assembly process and in the thermodynamic and kinetic stability of ring-closed structures when compared to linear assemblies.

The ^{1}H NMR spectra of **GC** in chlorinated solvents displayed a single set of proton resonances which are characteristic of G–C association (Figure 2a). The hydro-

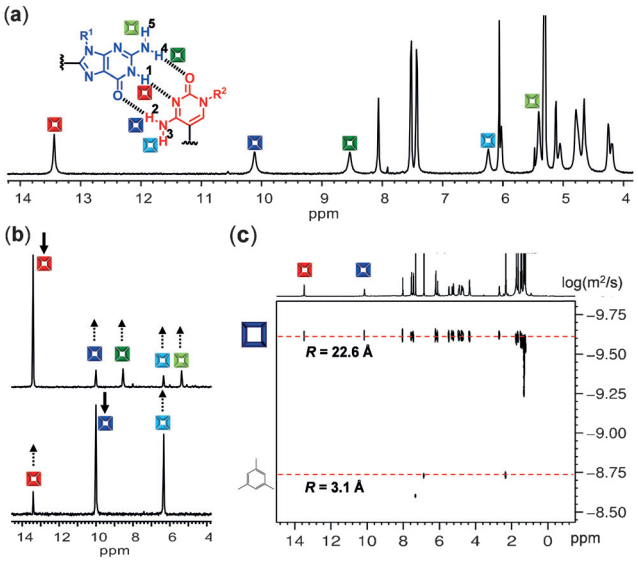

Figure 2. a) ^{1}H NMR spectrum of **GC** in CD_2Cl_2 at 248 K. All the amide and amine proton signals are shown. b) One-dimensional NOE spectra of **GC** in $CDCl_3$ at 298 K with irradiation of the G-H^1 signal (top) and the C-H^2 signal (bottom). c) DOSY NMR spectrum of **GC** in $CDCl_3$ at 298 K. In all cases $c = 10^{-2}$ M.

gen-bonded G-H^1 amide and the C-H^2 amine signals are found at $\delta = 13.4$ and 10.0 ppm, respectively. The C-H^3 signal was found around $\delta = 8$–6 ppm, depending on the solvent used (see Figure S1 in the Supporting Information). In contrast, the G-amine protons are found as a broad coalesced signal at 298 K and splits into two sharp signals at $\delta = 8.5$ (H^4) and 5.4 (H^5) ppm below 273 K (see Figure 2a and Figure S2).[15] One- and two-dimensional NOE experiments (see Figure 3b and Figure S3) showed crosspeaks between the hydrogen-bonded G-H^1 and C-H^2 protons, hence confirming G–C association.

It is interesting to note that the shape and position of the hydrogen-bonded G-H^1 and C-H^2 proton signals in **GC** are virtually not sensitive to concentration (10^{-1}–10^{-4} M; see Figure S4), temperature (223–373 K; see Figure S2) or solvent changes ($CDCl_3$, CD_2Cl_2, $CDCl_2CDCl_2$, [D$_8$]THF, [D$_6$]acetone; see Figure S1). This behavior is in sharp contrast to the behavior of the **G-C** 1:1 complex, whose signals are quite sensitive to these experimental changes, and suggests that a particularly stable supramolecular entity is formed by **GC**. In accordance, DOSY experiments in $CDCl_3$ within the 10^{-2} M to 10^{-4} M concentration range suggested the presence of a single species with a diffusion coefficient that is consistent with the hydrodynamic radius expected for c**GC**$_4$ (see Figure 2c and Figure S5). ESI Q-TOF mass spectrometry experi-

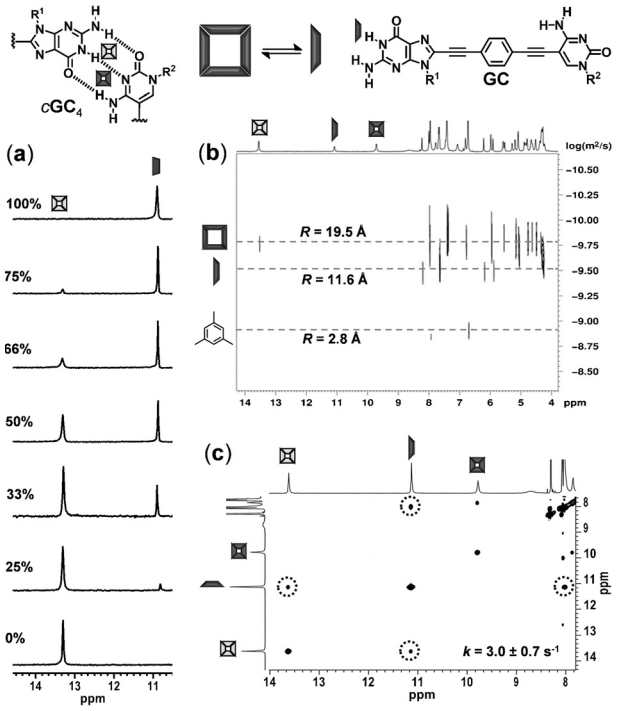

Figure 3. a) Amide region of the ^{1}H NMR spectrum of **GC** in $CDCl_3$/[D$_6$]DMSO solvent mixtures as a function of the DMSO content (v/v%). Dissociation of c**GC**$_4$ is observed. b) DOSY NMR spectrum of **GC** in [D$_7$]DMF showing the **GC** and c**GC**$_4$ signals with different diffusion coefficients. c) Amide region of the EXSY spectrum of **GC** in [D$_7$]DMF at a 200 ms mixing time. $c = 10^{-2}$ M; $T = 298$ K.

ments also sustained the formation of a tetramer (see Figure S6), and we could detect the singly, doubly, and triply charged **GC**$_4$ peaks and some of its fragments.[14]

To shed more light onto the structural nature and the thermodynamic and kinetic characteristics of c**GC**$_4$ in solution, we devised several experiments aimed to dissociate it. Because of its unusual stability, when compared for instance with the 1:1 **G–C** pair, we employed three drastic approaches: a) the use of very polar solvents such as [D$_6$]DMSO or [D$_7$]DMF, which are able to strongly compete for hydrogen bonding, in NMR experiments; b) optical spectroscopy experiments at very low concentrations and; c) competition experiments with mononucleoside stoppers.[13]

In contrast to the NMR solvents previously mentioned, the ^{1}H NMR spectrum of **GC** in [D$_6$]DMSO exhibited G-H^1 and C-H^2 proton signals at $\delta = 10.8$ and 7.9 ppm, and they are attributed to the solvent-bound **GC** monomer. The increase of the DMSO content in $CDCl_3$/[D$_6$]DMSO solvent mixtures resulted in the progressive dissociation of c**GC**$_4$. However, three main points should be noted in these experiments that differ significantly from the behavior of the 1:1 **G–C** complex (see Figure 3a and Figure S7): 1) the associated c**GC**$_4$ can resist large amounts of DMSO (it persists even at 80% v/v), which is quite notable for a hydrogen-bonded assembly; 2) the monomer–tetramer exchange seems to be very slow in the NMR timescale under these reaction conditions, since the shape and position of all signals do not change throughout the whole experiment and; 3) an all-or-nothing behavior was

noted, meaning that no other intermediate supramolecular species was detected (it is either $c\mathbf{GC}_4$ or **GC**, but nothing else). In [D_7]DMF a similar behavior was observed, but dissociation was not completed even in 100% [D_7]DMF.[14]

At a 10^{-2} M **GC** concentration, the use of a 1:1 $CDCl_3$/[D_6]DMSO mixture or pure [D_7]DMF resulted in an approximately 1:1 **GC**/$c\mathbf{GC}_4$ equilibrium mixture that was studied further. DOSY experiments indicated the presence of two diffusing species (see Figure 3b and Figure S8): one of them assigned to $c\mathbf{GC}_4$, with lower diffusion coefficients, and the other one to the **GC** monomer. The **GC**–$c\mathbf{GC}_4$ exchange kinetics was studied by EXSY in [D_7]DMF (see Figure 3c and Figure S9). From these experiments we could calculate the exchange rate constant ($k = 3.0 \pm 0.7\ s^{-1}$), and hence confirm that the **GC**–$c\mathbf{GC}_4$ exchange is remarkably slow even in this polar solvent, which underlines the high kinetic stability of the cyclic ensemble. In dilution experiments from 10^{-1} to 10^{-4} M (see Figure S10) or in cooling experiments from 323 to 273 K (see Figure S11) we could monitor the **GC**–$c\mathbf{GC}_4$ equilibrium. Again, no sign of any other species was found in these experiments, thus highlighting the cooperative nature of the cyclic assembly process. Since the exchange is very slow, we could derive the equilibrium constants (K_T) by signal integration (Table 1), and confirm that a tetramerization process holds for the whole range of concentrations and temperatures in both polar solvent systems.[16] A van't Hoff analysis of the temperature-dependent data afforded the thermodynamic parameters ΔH and ΔS (Table 1).

A second method we devised to study the **GC**–$c\mathbf{GC}_4$ equilibrium was the use of lower concentrations (10^{-4}–10^{-6} M) and more-sensitive techniques like absorption, emission, and circular dichroism (CD) spectroscopy as a function of concentration and temperature (Figure 4). Here, the choice of solvent was critical (see Figure S12). We found that solvents of intermediate polarity, like THF or 1,4-dioxane,[14] are ideal media to study these equilibria. When the chiral monomers associate in a cyclic tetramer assembly at high concentrations or low temperatures, a red-shifted absorption shoulder at $\lambda = 393$ nm, red-shifted emission maxima and, significantly, a Cotton CD effect arising with maxima at $\lambda =$ 357 and minima at $\lambda = 299$ and 404 nm were evidenced. Both

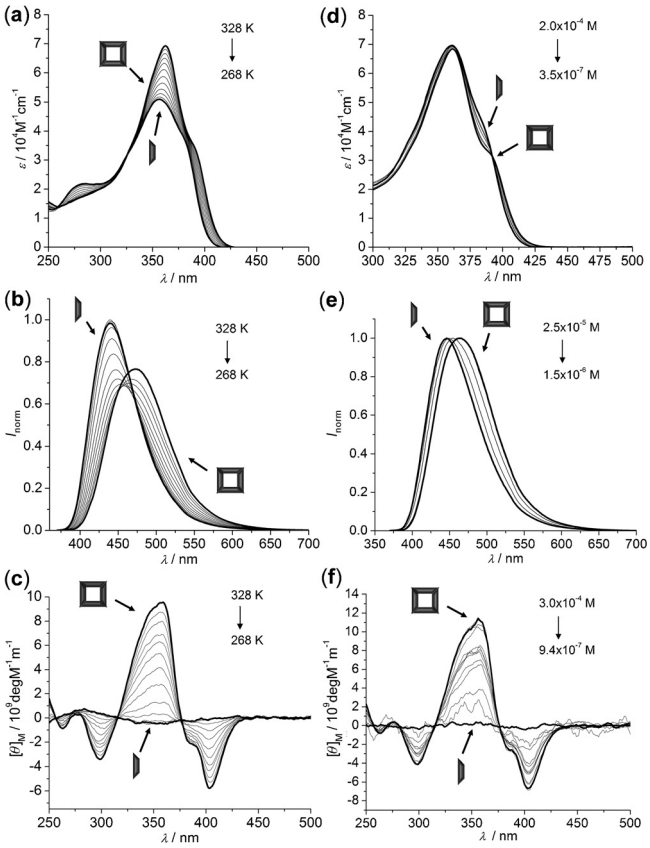

Figure 4. Absorption (a,d), emission (b,e), and CD changes (c,f) of **GC** in THF with temperature (a–c; $c = 1.25 \times 10^{-5}$ M) and concentration (d–f; $T = 298$ K) changes.

temperature- and concentration-dependent data were fitted to suitable models[14] to obtain the relevant thermodynamic parameters in THF (K_T, ΔH, and ΔS; see Figure S13 and Table 1).

Finally, a third way in which we studied $c\mathbf{GC}_4$ dissociation consists of the addition of a competitor for hydrogen bonding. We know so far that the **GC**–$c\mathbf{GC}_4$ equilibrium is very slow and shifted to the tetramer. Now, if we add increasing amounts of **C**, it will compete with the **GC** monomer for binding to the G units in $c\mathbf{GC}_4$, and thus gradually shift the equilibrium towards a **GC·C** complex. We were able to monitor this competition at different **GC** concentrations in $CHCl_3$, THF, and DMF by both ^{1}H NMR and fluorescence titration experiments (Figure 5).

As evidenced in ^{1}H NMR titrations (see Figure 5a and Figure S14), the addition of **C** to a solution of $c\mathbf{GC}_4$ results in the gradual disappearance of the $c\mathbf{GC}_4$ proton signals and the emergence of a new set of signals attributed to the **GC·C** complex, in fast equilibrium with

Table 1: Thermodynamic parameters obtained for the **GC** tetramerization process in different solvents.

Solvent	K_{ref} [M^{-1}]	K_T [M^{-3}]	EM [M]	ΔH [kJ mol^{-1}]	ΔS [J mol^{-1} K^{-1}]
DMF	5.7 ± 0.3[a]	$(2.3 \pm 0.8) \times 10^5$[c]	218	-155 ± 38[h]	-425 ± 94[h]
		$(3.8 \pm 2.4) \times 10^5$[d]	357		
THF	$(1.5 \pm 0.1) \times 10^3$[a]	$(1.0 \pm 0.2) \times 10^{15}$[e]	197	-225 ± 44[f]	-465 ± 126[f]
		$(2.2 \pm 1.8) \times 10^{15}$[f]	434		
		$(2.7 \pm 1.5) \times 10^{15}$[d]	526		
		$(2.1 \pm 0.3) \times 10^{15}$[g]	414		
$CHCl_3$	$(2.8 \pm 0.3) \times 10^4$[b]	$(5.6 \pm 3.1) \times 10^{20}$[d]	910		
		$(5.0 \pm 0.1) \times 10^{20}$[g]	813		

[a] Titration with **G** and **C** (see Figure S15). [b] Determined in Ref. [13]. [c] Dilution in [D_7]DMF (see Figure S10). [d] NMR competition experiments (see Figure S14). [e] Dilution in THF (see Figure S13). [f] Temperature experiments in THF (see Figure S13). [g] Fluorescence competition experiments (see Figure S14). [h] Temperature experiments in [D_7]DMF (see Figure S11).

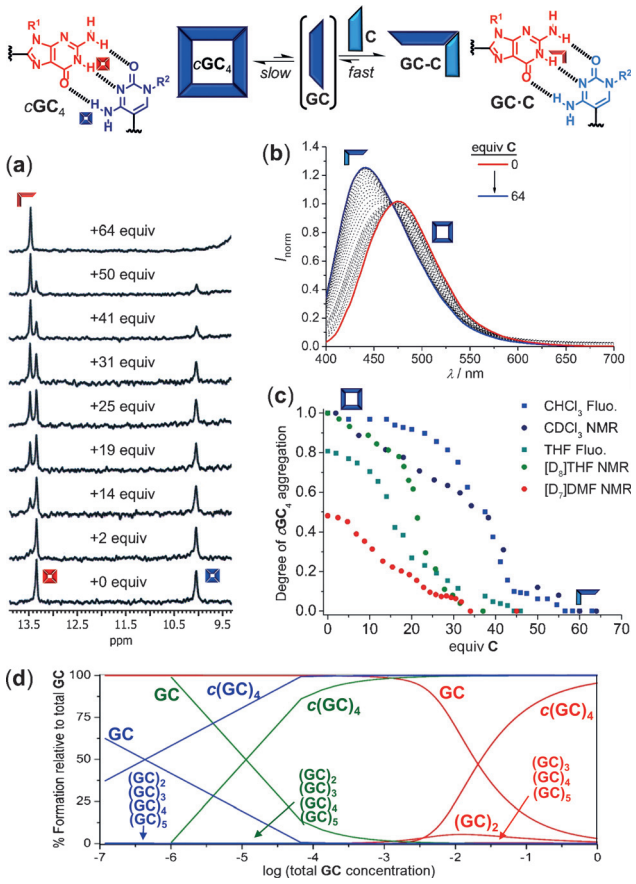

Figure 5. Titration experiments of **GC** with **C** at 298 K. a) Change in the ^{1}H NMR data ($c = 10^{-3}$ M in $CDCl_3$). b) Normalized fluorescence emission changes ($c = 5 \times 10^{-5}$ M; $\lambda_{exc} = 390$ nm) in $CHCl_3$. c) Plots of the degree of $c\mathbf{GC}_4$ association, measured by either ^{1}H NMR spectroscopy or emission, as a function of the equivalents of **C** added. d) Speciation profiles including the **GC**, $\mathbf{GC}_2$, $\mathbf{GC}_3$, $\mathbf{GC}_4$, $\mathbf{GC}_5$, and $c\mathbf{GC}_4$ species. Solvent codes (for c,d): DMF (red), THF (green) and $CHCl_3$ (blue).

excess **C**. It is significant to note again that $c\mathbf{GC}_4$ is in slow exchange with the other species in solution, and allowed us to determine their relative concentrations by integration. In emission experiments (see Figure 5b and Figure S14), a blue-shift was monitored as $c\mathbf{GC}_4$ is dissociated with excess **C**. Actually, in these experiments the intra- and intermolecular G–C binding events compete, so we could directly calculate K_T from the relevant equilibrium constants (Table 1).[14] Figure 5c shows the competition trends in the three solvents. To fully dissociate $c\mathbf{GC}_4$ one must reach about 60 ($CHCl_3$), 40 (THF), or 35 (DMF) **C** equivalents,[18] which underlines the stability of the cyclic assembly.

From the different K_T values obtained and the reference G–C association constants (K_{ref}) determined by titration experiments with **G** and **C** (see Figure S15), we could estimate the EM in each of the three solvents employed (Table 1) by using the relationship: $K_T = K_{ref}{}^4 \cdot EM$.[17] The product $K_{ref}{}^4 \cdot EM$ is considerably enhanced in low polarity media and in all cases exceeds $185 \cdot n$, (n being the number of monomers in the cycle; $n = 4$), a condition defined by Ercolani to reach complete cycle assembly at a given monomer concentration.[8b] The speciation profiles simulated in each solvent (Figure 5d) satisfactorily reproduce our experimental results and illustrate that $c\mathbf{GC}_4$ can be formed quantitatively in a wide range of concentrations, as long as the binding constant is kept high enough through low solvent competition for G–C hydrogen bonding. The lower self-assembly concentration (*lsac*),[8b] that is, the concentration at which half of the monomer is assembled into macrocycles, was estimated as: $lsac^{DMF} = 1.6 \times 10^{-2}$ M, $lsac^{THF} = 9.5 \times 10^{-4}$ M, and $lsac^{CHCl3} = 4.1 \times 10^{-7}$ M (see also Figure 5d).[14]

This work reveals the consequences of optimal monomer design on the fidelity of a supramolecular oligomerization process towards a specific macrocyclic structure. $c\mathbf{GC}_4$ exhibits an impressive thermodynamic stability and constitutes a kinetically steady product in the overall self-assembly landscape, even in highly polar solvents, where hydrogen-bonded association is typically too weak. Both monomer structure and binding interaction geometry and nature have to be considered to produce cyclic species devoid of strain and with minimal conformational entropy loss. This was achieved on one hand by employing a rigid monomer with only four rotatable linear π-conjugated bonds. Rotation around these bonds, however, is not restrained upon self-assembly. The only degree of freedom that is lost upon cycle formation, when compared to open oligomers, is the relative conformational arrangement between nucleobases. $c\mathbf{GC}_4$ demands all Watson–Crick edges to be in a *syn* conformation but an open structure is free to alternate between *anti* and *syn* conformations (Figure 1). On the other hand, $c\mathbf{GC}_4$ assembles through three hydrogen-bonding interactions, which is relatively strong and asymmetric (DDA-AAD pattern), and directs association with a well-defined 90° angle. We believe that the rigidity and non-rotatable nature of this multipoint binding interaction is a key factor that notably increases the magnitude of EM in $c\mathbf{GC}_4$ (10^2–10^3 M)[17,18] when compared to other cyclic tetramers based on metal–ligand interactions (EM = 0.1–20 M).[10] Our results underscore the use of multiple hydrogen-bonding interactions, in this case DNA bases, to enhance chelate cooperativity to produce a target assembly with high fidelity.

Keywords: chelates · noncovalent interactions · nucleosides · self-assembly · supramolecular chemistry

How to cite: *Angew. Chem. Int. Ed.* **2015**, *54*, 6780–6784
Angew. Chem. **2015**, *127*, 6884–6888

[1] L. J. Prins, D. N. Reinhoudt, P. Timmerman, *Angew. Chem. Int. Ed.* **2001**, *40*, 2382–2426; *Angew. Chem.* **2001**, *113*, 2446–2492.
[2] M. Iyoda, J. Yamakawa, M. J. Rahman, *Angew. Chem. Int. Ed.* **2011**, *50*, 10522–10553; *Angew. Chem.* **2011**, *123*, 10708–10740.
[3] P. Ballester, J. de Mendoza, in *Modern Supramolecular Chemistry* (Eds.: F. Diederich, P. J. Stang, R. R. Tykwinski), Wiley-VCH, Weinheim, **2008**, pp. 69–111.
[4] S. Höger, *Angew. Chem. Int. Ed.* **2005**, *44*, 3806–3808; *Angew. Chem.* **2005**, *117*, 3872–3875.
[5] a) C. A. Hunter, H. L. Anderson, *Angew. Chem. Int. Ed.* **2009**, *48*, 7488–7499; *Angew. Chem.* **2009**, *121*, 7624–7636; b) G. Ercolani, L. Schiaffino, *Angew. Chem. Int. Ed.* **2011**, *50*, 1762–1768; *Angew. Chem.* **2011**, *123*, 1800–1807.
[6] Focus Issue on Cooperativity: *Nat. Chem. Biol.* **2008**, *4*, 433–507.

[7] L. Mandolini, *Adv. Phys. Org. Chem.* **1986**, *22*, 1 – 111.
[8] a) X. Chi, A. J. Guerin, R. A. Haycock, C. A. Hunter, L. D. Sarson, *J. Chem. Soc. Chem. Commun.* **1995**, 2563 – 2565; b) G. Ercolani, *J. Phys. Chem. B* **1998**, *102*, 5699 – 5703; c) G. Ercolani, *J. Phys. Chem. B* **2003**, *107*, 5052 – 5057; d) G. Ercolani, *Struct. Bond.* **2006**, *121*, 167 – 215.
[9] The influence of different factors on chelate cooperativity has been analyzed. See: a) C. A. Hunter, M. C. Misuraca, S. M. Turega, *J. Am. Chem. Soc.* **2011**, *133*, 20416 – 20425; b) M. C. Misuraca, T. Grecu, Z. Freixa, V. Garavini, C. A. Hunter, P. van Leeuwen, M. D. Segarra-Maset, S. M. Turega, *J. Org. Chem.* **2011**, *76*, 2723 – 2732; c) H. J. Hogben, J. K. Sprafke, M. Hoffmann, M. Pawlicki, H. L. Anderson, *J. Am. Chem. Soc.* **2011**, *133*, 20962 – 20969; d) C. A. Hunter, M. C. Misuraca, S. M. Turega, *Chem. Sci.* **2012**, *3*, 589 – 601; e) C. A. Hunter, M. C. Misuraca, S. M. Turega, *Chem. Sci.* **2012**, *3*, 2462 – 2469; f) H. Adams, E. Chekmeneva, C. A. Hunter, M. C. Misuraca, C. Navarro, S. M. Turega, *J. Am. Chem. Soc.* **2013**, *135*, 1853 – 1863; g) H. Sun, C. A. Hunter, C. Navarro, S. Turega, *J. Am. Chem. Soc.* **2013**, *135*, 13129 – 13141.
[10] For other cyclic tetramer assemblies whose EMs have been calculated, see: a) X. Chi, A. J. Guerin, R. A. Haycock, C. A. Hunter, L. D. Sarson, *J. Chem. Soc. Chem. Commun.* **1995**, 2567 – 2569; b) G. Ercolani, M. Ioele, D. Monti, *New J. Chem.* **2001**, *25*, 783 – 789; c) I.-W. Hwang, T. Kamada, T. K. Ahn, D. M. Ko, T. Nakamura, A. Tsuda, A. Osuka, D. Kim, *J. Am. Chem. Soc.* **2004**, *126*, 16187 – 16198.
[11] For other hydrogen-bonded cyclic tetramer assemblies in solution, see: a) C. Nuckolls, F. Hof, T. Martín Jr., J. Rebek, *J. Am. Chem. Soc.* **1999**, *121*, 10281 – 10285; b) H. Ohkawa, A. Takayama, S. Nakajima, H. Nishide, *Org. Lett.* **2006**, *8*, 2225 – 2228; c) E. Orentas, C.-J. Wallentin, K.-E. Bergquist, M. Lund, E. Butkus, K. Wärnmark, *Angew. Chem. Int. Ed.* **2011**, *50*, 2071 – 2074; *Angew. Chem.* **2011**, *123*, 2119 – 2122; d) Y. Yang, M. Xue, L. J. Marshall, J. de Mendoza, *Org. Lett.* **2011**, *13*, 3186 – 3189.
[12] For the use of nucleobases in supramolecular chemistry: a) S. Sivakova, S. J. Rowan, *Chem. Soc. Rev.* **2005**, *34*, 9 – 21; b) J. L. Sessler, C. M. Lawrence, J. Jayawickramarajah, *Chem. Soc. Rev.* **2007**, *36*, 314 – 325.
[13] J. Camacho-García, C. Montoro-García, A. M. López-Pérez, N. Bilbao, S. Romero-Pérez, D. González-Rodríguez, *Org. Biomol. Chem.* **2015**, *13*, 4506 – 4513.
[14] See the Supporting Information for further details.
[15] a) D. González-Rodríguez, J. L. J. van Dongen, M. Lutz, A. L. Spek, A. P. H. J. Schenning, E. W. Meijer, *Nat. Chem.* **2009**, *1*, 151 – 155; b) D. González-Rodríguez, P. G. A. Janssen, R. Martín-Rapún, I. De Cat, S. De Feyter, A. P. H. J. Schenning, E. W. Meijer, *J. Am. Chem. Soc.* **2010**, *132*, 4710 – 4719.
[16] Cyclic trimer or pentamer assemblies were not properly fitted by the different methods employed in this work. Molecular modeling studies at the PM3 level (see Figure S5) show that these structures are more strained and far from achieving an optimal G–C hydrogen-bonding geometry. Moreover, cyclic tetramer assemblies were observed by STM studies over HOPG, which will be the subject of a forthcoming publication.
[17] The competition trends and the calculated EM values seem to reveal a relationship between EM and binding strength (K_{ref}), modulated by the solvent. Further studies will be performed to address this issue.
[18] To the best of our knowledge, this is the first example of a hydrogen-bonded cyclic tetramer whose EM values were calculated, so we could not make a direct comparison. A cyclic trimer, assembled through two hydrogen-bonding interactions, was reported to have EM values of 760 M. See Ref. [3] and: a) S. C. Zimmerman, B. F. Duerr, *J. Org. Chem.* **1992**, *57*, 2215 – 2217. On the other hand, a related ethenylene-bound G-C monomer has been reported by the Sessler's group to produce instead trimeric macrocycles: b) J. L. Sessler, J. Jayawickramarajah, M. Sathiosatham, C. L. Sherman, J. S. Brodbelt, *Org. Lett.* **2003**, *5*, 2627 – 2630.

Received: February 10, 2015
Published online: April 17, 2015

